OXIDATION-REDUCTION BEHAVIOURS, ELECTROLYSIS CHARACTERISTICS AND EFFICIENCY OF Pd-50at.%Ni ELECTRODE IN ALKALINE ELECTROLYTE

MD. ASHRAFUL ISLAM MOLLA, MITHUN SARKER, RAFIQUL ISLAM

Department of Applied Chemistry and Chemical Technology, Dhaka University,

Dhaka-1000, Bangladesh.

AND

A. K. M. FAZLE KIBRIA*

Chemistry Division, Atomic Energy Centre, P. O. Box-164, Ramna, Dhaka-1000, Bangladesh.

ABSTRACT

Convinced on the necessity of finding effective electrodes for electrolyser- the oxidation-reduction behaviors, surface reaction kinetics, stability, electrolysis characteristics and efficiency of a Pd-50at.%Ni electrode have been investigated in 30wt.%KOH electrolyte at room temperature using cyclic voltammetry. Cyclic voltammogram of the electrode showed three couples of oxidation-reduction peaks in between the potential range – 1.0 to + 0.65 V. These peaks were found to be originated from the transformation of zero valent metal to their higher oxides in three consecutive steps and vice versa. The peak potentials, potential differences of the couples and the peak currents were found remarkably different from those of Pd and Ni electrodes. The surface reaction kinetics at Pd-Ni electrode followed the surface reaction trends similar to those of Pd and Ni electrodes. The apparent stability of the electrode was found good. The electrode showed 1.6 and 6.8 times higher oxygen evolution efficiencies than the Ni and Pd electrodes. Addition of Ni with Pd caused hydrogen evolution potentials to move to the negative direction. Tafel plot for the hydrogen evolution reactions (HER) showed two well-defined Tafel regions. Kinetic parameters, i.e., Tafel slope and exchange current density values for the low and high overpotential regions were found 127 mV/dec and 273 mV/dec, and 1.72 x 10^{-2} mA/cm^2 and 1.52 mA/cm^2, respectively. Observed slopes indicated its better efficiency over the Pd electrode.

1. INTRODUCTION

To improve the capability of an industrial electrolyzer, the necessity of electrode materials with high catalytic properties are well known.(1) The aim of installing an electrolyzer is to produce enormous amounts of hydrogen and oxygen with high purity by electrochemical means for future applications. Pure hydrogen and oxygen are essential for fuel cell to produce electricity, pure hydrogen for automotive vehicles instead of fossil fuels and metal hydride battery for light electronic instruments.(1,2) Pure gases are very essential to avoid poisoning of electrode materials. In view of the depletion and pollution aspects of fossil fuels and ozone depletion trends of conventional refrigerants, hydrogen

* Corresponding author

is believed to be the future fuel and air conditioning medium. Hydrogen can also be used in household works in lieu of natural gas.

Hydrogen and oxygen evolution reactions are the basic cathodic and anodic reactions of an electrolyzer. Their generation mechanisms are different from one electrode to another. The electrolysis capability of an electrode depends on various factors.[3] There is no material that can cover all the criterion of a standard electrode. For a number of decades, researchers have been contributing to improve electrode materials for electrolyzer. Although a lot of improvements of electrodes has been made but this route of hydrogen and oxygen production is expensive and therefore needs further research.[4] In order to find more effective electrodes, recently researchers have been concentrating on metal composites,[5] amorphous metals[6] and bimetallic materials and have tested the electrolysis performances of bimetallic electrodes like Co-Cu,[7] Ni-Cu,[8] Ni-Fe,[9] Ni-Co,[10] Pd-Ag,[11] Pd-P,[12] etc.

The surface behavior and the electrolysis efficiency of Pd[13] and Ni[14-16] electrodes are fairly well known. Pd electrode is capable of evolving hydrogen at lower potentials than Ni. But it requires higher potentials than Ni to evolve oxygen. Pd-Ni alloy may therefore be a good electrocatalyst for both the hydrogen and oxygen evolutions at lower potentials than its components. This view encouraged us to investigate the electrochemical behavior of a Pd-Ni electrode. Study on Pd-Ni electrode is very limited. Recently, authors[17] have investigated on the M(II) ↔ M(III) transformation characteristics of a Pd-Ni electrode having Pd mol%63 and Ni mol%37 in a small potential range 0 to 0.65 V RHE.

It is well known that when the precursor components of an alloy establish a solid solution, it rarely retains the crystallographic structure of its components. As a result, the potentials of surface reaction steps and the corresponding peak currents of an alloy electrode differ remarkably from those of the component single metal electrodes. Pd and Ni establish a solid solution in all ranges of composition.[17,18] In this situation, some distinct behavior of Pd-Ni electrode different from those of Pd and Ni electrodes can be expected. Specially, there may appear the predomination of Pd over Ni or vice versa. Such a behavior of Pd-Ni electrode may provide better electrocatalytic activity for electrolysis. In this context, the present investigations attempt to find out the significant differences in electrochemical surface reaction behaviors, hydrogen and oxygen evolution characteristics and efficiencies, surface reaction kinetics, etc., of a Pd-Ni alloy relatives to those of its components Pd and Ni. Alkaline electrolyte medium is chosen because of having better corrosion resistance capability of Pd and Ni in this medium than in the acidic medium.[12,14]

2. EXPERIMENTAL

Pd-50at.%Ni alloy was prepared by non-consumable arc melting in argon atmosphere in the Nagasaki University Research Laboratory, Japan, by using 99.9% pure Pd and Ni purchased for National Hydrogen Energy (NHE) project of Japan. The alloy ingot was then annealed at 973 K in vacuum. It was then rolled into a plate of 1 mm thickness. The plate was then cut into square size to prepare the working electrode. It was then spot welded with a nickel wire. The lower part of the connecting wire was then insulated by a pyrex glass pipe and epoxy resin. The surface area of the electrode is 0.76 cm^2. A nickel plate of thickness 1 mm and surface area 9.25 cm^2 was prepared, spot welded with nickel wire and then insulated to use it as counter electrode. To remove any

oxides present on the surface of the electrodes, these were chemically etched. The surfaces of the electrodes were then polished by a cloth having alumina grain paste and subsequently rinsed with deionized water. The used electrolyte was 30wt.%KOH solution. It was prepared from the reagent grade KOH pellets.

A three-electrode cylindrical electrochemical cell designed and developed in the electrochemistry laboratory, Atomic Energy Centre, Dhaka, was used for the experimental measurements. The indigenously prepared working electrode, counter electrode and the $Hg/HgO.OH^-$ (E = – 0.926 V vs. RHE) reference electrode were immersed in 100 ml electrolyte in triangular way. The luggin capillary end of the reference electrode was placed approximately 2 mm apart from the surface of the Pd-50at.%Ni working electrode in order to minimize the internal resistance (IR) of the cell. The electrolyte was then made free from dissolved oxygen by bubbling N_2 gas for 30 minutes. Cyclic voltammetric measurements of the electrode were carried out by EG&G PARC Model 362 potentiostat/Galvanostat and potential-current responses were drawn by EG&G PARC Model RE 0089 X-Y recorder.

The electrode was activated initially by maintaining a cathodic potential – 1.0 V for 30 minutes. The surface reaction behaviors, i.e., the oxidation-reduction processes of the electrode materials and the hydrogen and oxygen evolution characteristics of the alloy were investigated in between the potential range – 1.0 to + 0.65 V by applying a potential sweep rate 100 mV/s. The chosen potential range was found sufficient to realize the acceptable surface reactions along with the hydrogen and oxygen evolutions. It is clearly described in the result and discussion part. It is notable that a wider potential range than the chosen one could only increase the evolutions of hydrogen and oxygen in the cathodic and anodic regions, respectively.

In order to understand the surface reaction kinetics, potential sweep rates 20 to 200 mV/s were applied. For the determination of the kinetic parameters, i.e., Tafel slope, b, overpotential, η, and exchange current density, i_o, of the hydrogen evolution reaction (HER), continuous potential sweep method was used. Potential sweeps were carried out by varying the cathodic potential 0.02 V in each scan towards positive potential direction from – 1.50 V with a sweep rate of 10 mV/s. It was done to evaluate the hydrogen evolution efficiencies at different cathodic potentials in view to draw the Tafel plot (potential vs current plot). The final positive potential was 0 V. The experiments were carried out at room temperature.

3. RESULTS AND DISCUSSION

Figure 1 shows the cyclic voltammogram appeared for the Pd-50at.%Ni electrode in 30wt.%KOH electrolyte in between the potential range – 1.0 V to + 0.65 V at room temperature at the sweep rate 100 mV/s. From the voltammogram, it is clear that the electrode surface materials suffered three oxidation and three reduction steps. The peaks originated by the oxidation steps are represented as $p_{a1,}$ p_{a2} and p_{a3} and those generated by the reduction are $p_{c1,}$ p_{c2} and p_{c3}. Potentials of the oxidation peaks are – 0.74 V, 0.05 V and 0.46 V, and those of reduction peaks are – 0.77 V, – 0.38 V and 0.37 V, respectively. By analyzing the observed peak potentials, it may be speculated that peaks p_{a1} and p_{c1}, peaks p_{a2} and p_{c2}, and peaks p_{a3} and p_{c3} are couple of oxidation-reduction peaks. Considering the peak potentials and valency of the alloy components, it may be assumed that peaks p_{a1} and p_{c1} originated from the oxidation-reduction of zero valent metal surface to metal(II)oxide and vice versa. Hydrogen and oxygen evolutions appeared in the

voltammogram near the negative and positive terminal ends by responding to the appreciable exerting driving potentials after following the required reaction steps of the electrode processes. It can be seen that adsorption of hydrogen on the surface of the electrode began at about the potential – 0.86 V.[13,14] Thus in the present experimental set up, hydrogen adsorption region can be considered from – 0.86 V to – 1.0 V.[12-15] Hydrogen evolution started instantly after reversal of potential towards the positive potential direction. Appearance of gas bubble confirmed the evolution of hydrogen gas.[7,13-15] Maximum current for the hydrogen evolution appeared at the set potential – 1.0 V and its value is 0.66 mA/cm^2. Hydrogen evolution current gradually decreased with decreasing the negative potential value and stopped just before the appearance of the oxidation peak p_{a1}.[13-16] On the other hand, maximum current for the oxygen evolution appeared at the set potential 0.65 V and it is 8.8 mA/cm^2. It is notable that the extent of hydrogen or oxygen evolution at a potential corresponds to the current appeared at that potential.[5,7] Current for the oxygen evolution sharply decreased with decreasing the positive potential values and finally reached to a minimum value at about the potential 0.56 V.[8,13,14] It is clear that the oxidation-reduction peaks p_{a1}, p_{a3}, p_{c2} and pc_3 showed remarkable currents whereas those of other two peaks are very small.

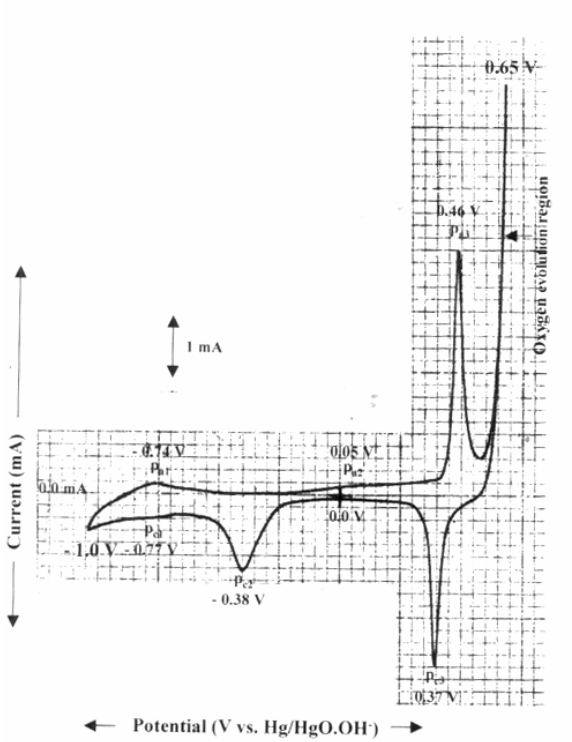

Figure 1. Cyclic voltammogram of Pd-50at.%Ni electrode in 30wt.%KOH electrolyte in between the potential range – 1.0 V to + 0.65 V at scan rate 100 mV/s.

Hydrogen and oxygen evolution reaction mechanisms are completely different.[5-8,19] There requires a number of surface reactions to evolve oxygen.[19] The most important

reaction is the formation of M(IV) oxide on the electrode surface. In the present case, the used electrode was in M(0) state. Here M represents Pd-Ni. So, at least three consecutive oxidation steps were mandatory to reach the surface into M(IV) oxide state. In these steps, loss of four electrons occurs from the electrode surface. It can be seen that oxidation of M(III) → M(IV) oxide began at about the potential 0.56 V. It is one electron process. Theoretically, its preceding oxidation peak marked by p_{a3} appeared due to the transformation of M(II) → M(III) oxide. This step is also a single electron process. Both the oxidation peaks p_{a2} and p_{a1} seem originated from the oxidation of the independent components of the alloy. These processes can be considered to be two-electron processes because of the possible transformation of the electrode surface from M(0) state to M(II) state. It seems that the oxidation peak p_{a3} originated from the participation of both the Pd(II) and Ni(II) oxides at a single potential value. The origin of the oxidation peaks p_{a2} and p_{a1} were found out and the techniques are described latter.

In order to find out whether the electrochemical surface reaction behaviors, hydrogen and oxygen evolution characteristics and efficiencies of Pd-50at.%Ni alloy were different from those of its components or not, cyclic voltammetric studies of Pd and Ni electrodes were carried out. Figure 2 shows the cyclic voltammogram observed for the Pd electrode. Three oxidation peaks p_{a1}, p_{a2} and p_{a3}, and two reduction peaks p_{c1} and p_{c2} appeared in the voltammogram. Inset figure shows the presence of peaks p_{a2} and p_{c2}. Potentials of the peaks are – 0.41 V, 0.34 V, 0.51 V, – 0.27 V and 0.25 V, respectively. The shape of the voltammogram is analogous to that reported for the same electrode in 0.1M KOH electrolyte at the scan rate 200 mV/s.[13] Peaks p_{a2} and p_{c1}, and p_{a3} and p_{c2} are couple of oxidation-reduction peaks. These originated from the transformations of Pd(0) ↔ Pd(II) oxide and Pd(II) oxide ↔ Pd(III) oxide, respectively. Oxidation of Pd(III) → Pd(IV) oxide began at about the potential 0.58 V. Oxygen evolution occurred due to its reduction and decomposition to Pd(III) oxide. The rest anodic peak p_{a1} appeared due to the desorption of diffusional hydrogen absorped in the Pd lattice.[13] Adsorption of hydrogen on the electrode surface began from about the potential – 0.58 V. Maximum hydrogen evolution occurred

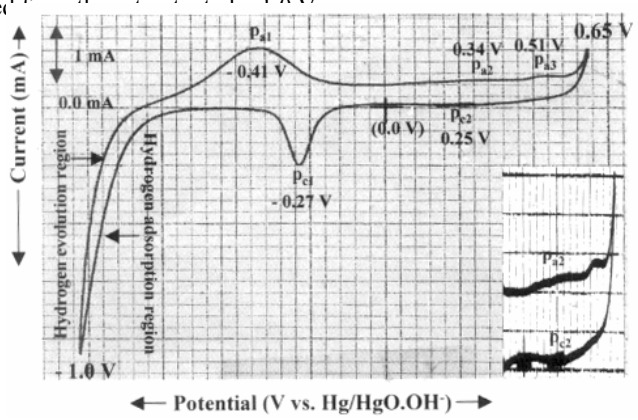

Figure 2. Cyclic voltammogram of Pd electrode in 30wt.%KOH electrolyte in between the potential range – 1.0 V to + 0.65 V at scan rate 100 mV/s. Inset figure shows the presence of peaks p_{a2} and p_{c2}.

Figure 3 shows the cyclic voltammogram appeared for the Ni electrode. A couple of oxidation-reduction peaks marked as p_{a1} and p_{c1} appeared at the potentials 0.48 V and 0.40 V. The part of the voltammogram having these peaks is analogous to that observed earlier for the same electrode and the peak potential values coincided with the reported values.[16,20] The peaks appeared due to the transformation of Ni(II) oxide ↔ Ni(III) oxide and showed remarkable currents. Transformation of Ni(III) → Ni(IV) oxide began at about the potential 0.57 V. Oxygen evolution occurred from the set potential + 0.65 V due to the reduction and decomposition of Ni(IV) → Ni(III) oxide.[19,20] Current for oxygen evolution decreased with decreasing potential. It can be seen that the set negative potential – 1.0 V was not enough to adsorb hydrogen and to commence hydrogen evolution. The observed result coincided with that reported earlier.[14] No remarkable peaks for Ni(0) ↔ Ni(II) oxide transformations were observed. In an earlier study, the peaks for these transformations were found at – 0.62 V and – 0.94 V after cycling a Ni electrode in between the potential – 1.1 V to – 0.3 V.[15] It indicates that in the present study, the set negative potential – 1.0 V was insufficient in getting these peaks. It seems that these peaks have close relationships with the couple of peaks p_{a1} and p_{c1} appeared for Pd-50at.%Ni electrode (Fig. 1) at potentials – 0.74 V and – 0.77 V, respectively.

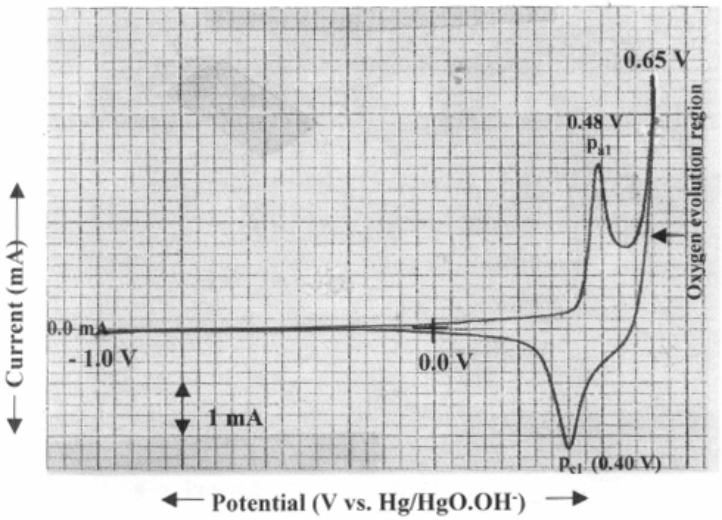

Figure 3. Cyclic voltammogram of Ni electrode in 30wt.%KOH electrolyte in between the potential range – 1.0 V to + 0.65 V at scan rate 100 mV/s.

Comparing the redox behavior of Pd-50at%Ni electrode (Fig. 1) with that of Pd and Ni electrodes (Figs. 2 & 3), it can be said that transformation of M(III) → M(IV) oxide began from about the same potential 0.56 V as those occurred for both the Pd(III) → Pd(IV) and Ni(III) → Ni(IV) oxides. Commencement of adsorption of hydrogen over the Pd-50at%Ni electrode surface moved about 0.28 V negative potential than that of Pd electrode. No remarkable anodic peak related to the p_{a1} of Pd electrode for the desorption of diffusional hydrogen from its lattice interstices appeared in the voltammogram. It occurred probably due to the decrease in lattice size of Pd-Ni alloy than that of Pd[21] and the presence of Ni(II) oxide layer over the zero valent Pd present on the Pd-50at.%Ni

electrode surface. Oxidation-reduction peaks p_{a2} and p_{c2} of Pd-50at.%Ni electrode seems to resemble the peaks p_{a2} and p_{c1} of Pd electrode which originated due to the Pd(0) ↔ Pd(II) transformations. The peaks moved to 0.29 V and 0.11 V negative potentials than those found for the Pd electrode. Ni related peaks for Ni(0) ↔ Ni(II) transformations moved to – 0.12 V negative potential and 0.17 V positive potential, respectively.[15] Pd related M(II) oxide ↔ M(III) oxide transformations are not pronounced in the voltammogram. Peak couple p_{a3} and p_{c3} of Pd-50at%Ni electrode seems to resemble the peak p_{a1} and p_{c1} of Ni electrode. The potentials of these M(II) oxide ↔ M(III) oxide transformation peaks are found about 0.02 V and 0.03 V negative potentials than those appeared for the transformations of Ni(II) oxide ↔ Ni(III) oxide. It indicates that the alloy components Pd and Ni are not completely showing their independent behavior during cycling. The component Ni predominates over the component Pd. Addition of Ni with Pd changed the redox potential of Ni and Pd related peaks remarkably.

From the observed oxidation-reduction behaviors of Pd-50at.%Ni electrode, the consecutive oxidation reaction steps and reaction paths can be represented as follows:

(i) First oxidation step: $M_{Ni} \rightarrow M_{Ni}O + 2e$ ……(1a)

$M_{Pd} \rightarrow M_{Pd}O + 2e$ ……(1b)

(ii) Second oxidation step: $MO \rightarrow M_2O_3 + e$ …….. (2)

(iii) Third oxidation step: $M_2O_3 \rightarrow M_2O_4 + e$ …… (3)

The next reaction step is the decomposition and simultaneous reduction of M_2O_4 to M_2O_3. An oxygen atom/half molecule of oxygen was produced from this reaction step, which then combined with other oxygen atom and produced oxygen molecule to evolve in gaseous form. Oxygen atoms combination step is known as Tafel step. The steps can be represented as:

(i) Reduction and decomposition step: $M_2O_4 \rightarrow M_2O_3 + 1/2O_2$ …… (4)

(ii) Tafel step : $1/2O_2 + 1/2O_2 \rightarrow O_2$ ……..…(5)

From the Fig. 1, it can be seen that current densities for the transformations of M(II) → M(III) oxide, Pd related M(0) ← M(II) oxide, hydrogen and oxygen evolutions are about 5.0, 1.3, 0.66 and 8.8 mA/cm^2, respectively. For the Pd electrode (Fig. 2), current densities for Pd(0) ← Pd(II) oxide transformation, hydrogen and oxygen evolutions are about 1.6, 7.2 and 1.3 mA/cm^2, respectively. In case of Ni electrode (Fig. 3), current densities for Ni(II) → Ni(III) oxide transformation and oxygen evolutions are 3.1 and 5.5 mA/cm^2. From the above findings, it is clear that Pd-50at.%Ni electrode showed more than 1.6 times higher current density than that of Ni(II) → Ni(III) transformation. It indicates the presence of higher amount of M(III) oxide layer on the surface of the Pd-50at.%Ni electrode than that on Ni electrode. This may happen due to the change in crystallographic structure of the Pd-Ni alloy from its components Ni and Pd.[3] Pd related M(0) ← M(II) transformation showed 0.8 times current density than that of Pd(0) ← Pd(II) transformation. It indicates the formation of lower amount of Pd(II) oxide layer on the surface of the Pd-50at.%Ni electrode than the Pd electrode. It seems reasonable because the amount of Pd in Pd-50.at%Ni electrode is lower than that of the Pd electrode. Hydrogen evolution current density is 10.9 times lower than that of Pd electrode but 100% higher than the Ni electrode. Oxygen evolution current density is 1.6 and 6.8 times

higher than those of Ni and Pd electrodes, respectively. These results are informing that M(II) oxide films grown over the Pd-50at.%Ni electrode surface are significantly oxidized to M(III) and then M(III) → M(IV) oxide.[8]

Figure 4 shows the cyclic voltammograms for Pd-50at.%Ni electrode at the scan rates of 20, 50, 100 and 200 mV/sec in between the potential range – 1.0 to + 0.65 V. It can be seen that the oxidation-reduction behaviors showed the same trends with the variation of scan rates. Peak currents gradually increased. The peak p_{a1} significantly moved to the positive direction and the peak p_{c1} moved to the negative potential direction. As a result, differences in peak potentials ΔEp_{11} gradually increased. The peak p_{c2} highly moved to the negative potentials and ΔEp_{22} gradually increased. Peaks p_{a3} and p_{c3} gradually moved to the positive potential direction by keeping their potential differences ΔEp_{33} same. Analogous movement of peaks relevant to p_{a1}, $p_{a3,}$ $p_{c1,}$ p_{c2} and p_{c3} were also observed on Pd and Ni electrode surfaces at different scan rates. Figure 5 shows the peak currents ($I_{pa,c}$) against square root of scan rates ($V^{1/2}$) relationships of the significant oxidation-reduction peaks: Pd(0) ← Pd(II) oxide, Ni(II) → Ni(III) oxide, Pd related M(0) ← M(II) oxide and M(II) → M(III) oxide of Pd, Ni and Pd-50at.%Ni electrodes. It can be seen that $I_{pa,c}$ values showed linear dependences with $V^{1/2}$. But none of them passed through the origin. It indicates that above oxidation-reduction reactions were not purely diffusion-controlled processes. Authors[17] have also reported similar trend of reaction for the transformation of M(II) → M(III) oxide of Pd-Ni electrode. The observed results are indicating that addition of Ni with Pd is not changing the trends of surface redox reaction kinetics.

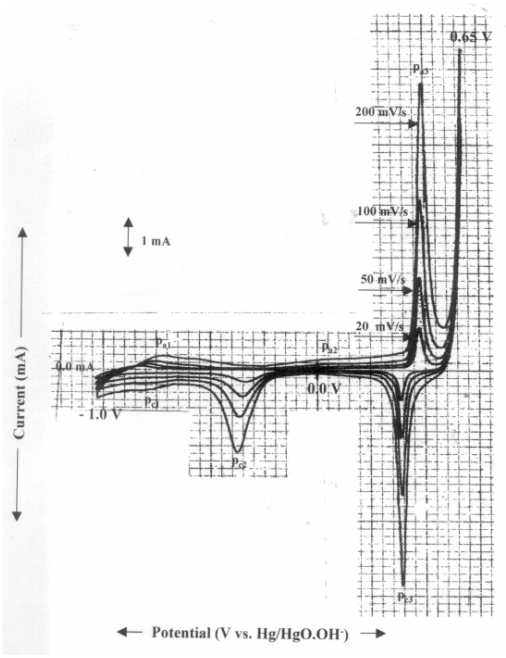

Figure 4. Cyclic voltammograms of Pd-50at.%Ni electrode in 30wt.%KOH electrolyte in between the potential range – 1.0 V to + 0.65 V at different scan rates.

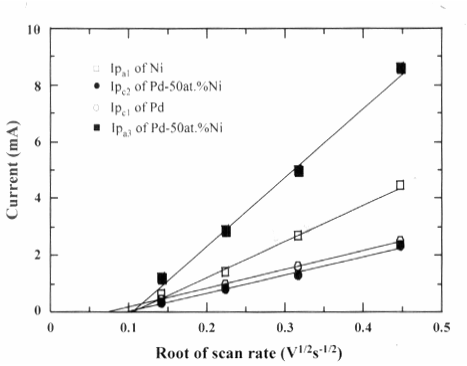

Figure 5. Dependence of peak currents with the square root of scan rates of Pd, Ni and Pd-50at.%Ni electrodes in 30wt.%KOH electrolyte.

Figure 6 shows the cyclic voltammograms obtained for Pd-50at%Ni electrode at 1, 3, 8, 15, and 25 minutes at scan rate of 200 mV/sec between the potential range – 1.0 to + 0.65 V. It can be seen that increase in currents for Ni releted M(0) ↔ M(II) oxide and Pd related M(0) → M(II) oxide transformations are not so significant. But currents for M(II) oxide ↔ M(III) oxide transformations are gradually increased with increasing time. It can be seen that two new reduction peaks marked by p_{c2*} and p_{c3*} appeared through the splitting of peaks p_{c2} and p_{c3} at about 0.31 V and – 0.27 V, respectively. These peaks probably appeared due to the reduction of ßPd(III) → ßPd(II) oxide and ßPd(II) → Pd(0), respectively. The observed peak splitting behaviors are different from the time dependent behaviors of Pd and Ni electrodes. Current for Pd related M(0) ← M(II) oxide transformation increased but it is not contributing in hydrogen evolution. Current densities for M(II) → M(III) oxide transformation at the recorded periods are 6.3, 7.4, 9.0, 10.5 and 12.1 mA/cm^2, respectively. Increase in current/min decreased with increasing time. Increase in current with time indicates that the thickness of M(III) oxide film over the electrode surface gradually increased. It means that the oxygen evolution efficiency of the electrode gradually increased with time. The observed behavior indicates that the apparent stability of the electrode is remarkable.[16,17]

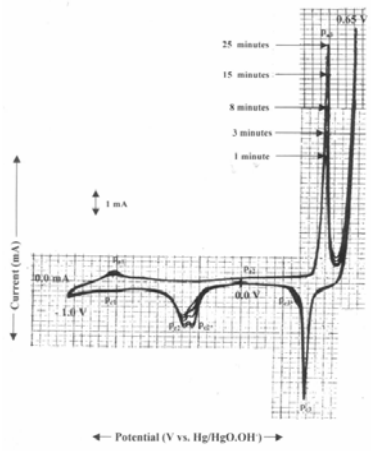

Figure 6. Cyclic voltammograms of Pd-50at.%Ni electrode at different times in 30wt.%KOH electrolyte in between the potential range – 1.0 V to + 0.65 V.

In order to understand the effect of variation of potential range on the redox behavior of Pd-50at.%Ni electrode, studies were carried out by fixing the negative potential at – 1.0 V and varying the positive potential from 0.60 V towards negative direction at scan rate 200 mV/sec. The cyclic voltammograms observed at various potential ranges are shown in Fig. 7. It can be seen that currents for oxygen evolution and that of M(II) oxide ↔ M(III) oxide gradually decreased with decreasing the potential range. Oxidation-reduction of M(II) and M(III) oxides disappeared at above the potential 0.40 V. Peak currents for the Pd related M(0) ← M(II) reduction process gradually decreased and the peak potentials gradually moved to the positive potential direction. It occurred due to the gradual decrease in oxidation of Pd related M(0) → M(II) oxide. Such a behavior was observed for Pd electrode while cycling at various potential ranges. It means that the surface of the electrode gradually freed from Pd(II) oxide layer. So, fraction of M(0) surface gradually increased but the surface still covered by Ni(II) oxide. This is the reason of the movement of hydrogen adsorption region of Pd-50at.%Ni electrode to the negative potential than the Pd electrode because hydrogen can't adsorp over an oxide layer. For it, M(0) surface is essential. However, it can be speculated that after achieving the M(0) surface, the electrode may show significant hydrogen evolution efficiency by showing better electrode reaction kinetics.

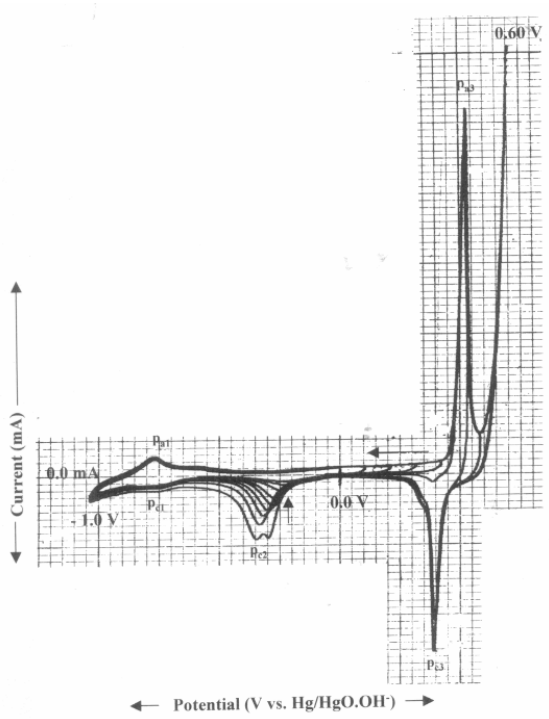

Figure 7. Cyclic voltammograms of Pd-50at.%Ni electrode in 30wt.%KOH electrolyte in between the potential ranges – 1.0 V and + 0.60 V.

In order to determine the kinetic parameters of the hydrogen evolution reactions (HER), hydrogen evolution currents (*i* values) at different potential ranges were determined after activating the electrode at – 1.50 V for 30 minutes. The investigated potential ranges were in between – 1.50 V to 0 V. The kinetic parameters- the exchange

current density (i_o) and Tafel slope (b), were found out from the Tafel plot drawn by plotting overpotential (η) against log$i$. Overpotential values were calculated by deducing the $Hg/HgO.OH^-$ reference electrode potential – 0.926 V from the working potentials. The Tafel plot is shown in Figure 8. It can be seen that the Tafel plot shows two well-defined Tafel regions as that observed for Ni,[15] Ni based alloy[10,14] and Pd based alloy.[11] The region at low overpotentials is known as low η region. For low η region, the i_o and b values are found 1.72 x 10^{-2} mA/cm^2 and 127 mV/dec. The region at high overpotentials is known as High η region. For this region the obtained i_o and b values are found 1.52 mA/cm^2 and 273 mV/dec. b values are calculated from the slopes of the Tafel lines. These values are known as experimental values. It was necessary to justify the experimental values with the calculated values. It is possible to calculate η values at a current density by putting the experimental values of i_o and b in the well known equation: $\eta_i = b \log_{10}(i/i_o)$.[15,20] For high η region, η value was calculated at the current density of 100 mA/cm^2 and for low η region, η value was calculated at the current density of 10 mA/cm^2. The calculated values are 351 mV and 497 mV and the experimental values are 351 mV and 496 mV, respectively. It indicates that the experimental observations are perfect. In an earlier study, we have found out the i_o and b values for the Pd electrode.[22] Presently observed i_o and b values of Pd-50at.%Ni electrode are lower than those of Pd electrode. It means addition of Ni with Pd decreased the b values. The b values for low and high η regions decreased 31 mV and 6 mV, respectively. High i_o value and low b value are the requirements of a better electrode. In this sense, it can be said that the perfo

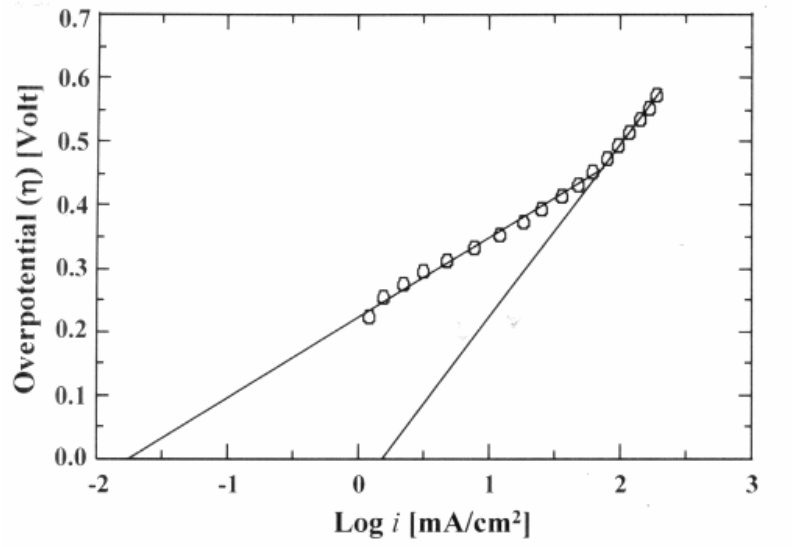

Figure 8. Tafel plot for the hydrogen evolution reactions (HER) over Pd-50at.%Ni electrode in 30wt.%KOH electrolyte at room temperature.

It is possible to propose the mechanism of the hydrogen evolution reaction (HER) over the Pd-50at.%Ni electrode surface. HER seems proceeded via three steps involving atomic hydrogen adsorption on the electrode surface namely water reduction with hydrogen adsorption known as Volmer step. To evolve hydrogen, two parallel competitive steps- electrochemical known as Heyrovsky step and chemical known as Tafel step followed the Volmer step. The reaction mechanisms can be represented as:

Volmer Step: $[M] + H_2O + e \rightarrow [M]H_{ads} + OH^-$ …… (1)

Heyrovsky Step: $[M]H_{ads} + H_2O + e \rightarrow H_2 + [M] + OH^-$ …….. (2)

Tafel Step: $[M]H_{ads} \rightarrow [M] + H_2$ ……..…….(3)

ACKNOWLEDGEMENTS

One of the authors is grateful to the Professor Yoshiichi Sakamoto, Department of Materials Science and Engineering, Nagasaki University, Japan, for supplying pure Pd plate and Pd-50at.%Ni alloy ingot.

REFERENCES

1. W. KREUTER AND H. HOFMAN, *Int. J. Hydrogen Energy,* **22**, 661, 1998.
2. H. AKI, S. YAMAMOTO, J. KONGOH, T. MAEDA, H. YAMAGUCHI, A. MURATA AND J. ISHII, *Int. J. Hydrogen Energy,* **31**, 967, 2006.
3. J. M. JAKSIC, N. V. KRSTAJIC, B. N. GRGUR, M. M. JAKSIC, *Int. J. Hydrogen Energy,* **23**, 667, 1998.
4. M. P. M. KANINSKI, D. L. STOJIC, D. P. SAPONJIC, N. I. POTKONJAK AND S. S. MILJANNIC, *J. Power sources,* **157**, 758, 2006.
5. Y. CHOQUETTE, L. BROSSARD, A. LAISA AND H. MENARD, *Electrochemica Acta,* **35**, 1251, 1990.
6. G. KREYSA AND B. HAKLANSSON, *J. Electroanal. Chem.,* **201**, 61, 1986.
7. L. BROSSARD AND B. MARQUIS, *Int. J. Hydrogen Energy,* **19,** 231, 1994.
8. A. K. M. F. KIBRIA AND S. A. TARAFDAR, *Int. J. Hydrogen Energy,* **27**, 879, 2002.
9. C. C. HU AND Y. R. WU, *Materials Chemistry and Phys.,* **82,** 588, 1993.
10. B. CHI, H. LIN, J. LI, N. WANG AND J. YANG, *Int. J. Hydrogen Energy,* **31**, 1210, 2006.
11. A. K. VIJH AND A. BELANGER, *Int. J. Hydrogen Energy,* **11**, 147, 1986.
12. J. J. PODESTA AND R. C. V. PIATTI, *Int. J. Hydrogen Energy,* **22**, 753, 1997.
13. M. M. JAKSIC, B. JOHANSEN AND R. TUNOLD, *Int. J. Hydrogen Energy,* **18**, 111, 1993.
14. M. J. DE. GIZ, J. C. P. DA. SILVA, M. FERREIRA, S. A. S. MACHADO, E. A. TICIANELLI, L. A. AVACA AND E. R. GONZALEZ, *Hydrogen Energy Progress,* **VIII**, 405, 1990.
15. M. F. KIBRIA, M. SH. MRIDHA, A. H. KHAN, *Int. J. Hydrogen Energy,* **20,** 435, 1995.
16. M. F. KIBRIA AND M. SH.MRIDHA, *Int. J. Hydrogen Energy,* **21,** 179, 1996.
17. L. J. VRACAR, S. BUROJEVIC AND N. KRSTAJIC, *Int. J. Hydrogen Energy,* **23**, 1157, 1998.

18. E. WICKE, H. BRODOWSKY AND H. ZUCHNER, "Hydrogen in Metals II", Springer, New York, 1978, pp. 223.

19. B. E. CONWAY, L. BAI AND M. A. SATTAR, *Int. J. Hydrogen Energy,* **12**, 607, 1987.

20. J. Y. HUOT AND L. BROSSARD, Int. J. Hydrogen Energy **12,** 821, 1987.

21. F. A. LEWIS, "The palladium hydrogen system, Academic press", 1967, pp. 71.

22. M. S. ISLAM, M. Sc. Thesis, Dhaka University, 2000.